

## Pharmacokinetics and Metabolism of <sup>14</sup>C-Brivaracetam, A Novel SV2a Ligand, in Healthy Subjects

Maria Laura Sargentini-Maier, Pascal Espié, Alain Coquette, Armel Stockis

*UCB Pharma SA, B-1420 Braine-l'Alleud, Belgium (MLSM, PE, AS)*

*SGS Healthcare Services SA, B-1301 Wavre, Belgium (AC)*

Corresponding author:

M.L. Sargentini-Maier

UCB Pharma SA, Chemin du Foriest,

B-1420 Braine-l'Alleud, Belgium

E-mail: [Laura.Maier@ucb-group.com](mailto:Laura.Maier@ucb-group.com)

Tel.: +32-2-3862789

Fax: +32-2-3862400

## Running title page

**Running title:** Pharmacokinetics and Metabolism of  $^{14}\text{C}$ -Brivaracetam

Address correspondence to: Dr M.L. Sargentini-Maier, UCB Pharma SA, Chemin du  
Foriest, B-1420 Braine-l'Alleud, Belgium. E-mail: [Laura.Maier@ucb-group.com](mailto:Laura.Maier@ucb-group.com).

Tel.: +32-2-3862789; Fax: +32-2-3862400

No. of pages: 27

No. of tables: 3

No. of figures: 5

No. of references: 13

No. of words in abstract: 217

No. of words in introduction: 295

No. of words in discussion: 598

**ABBREVIATIONS:** AUC, area under the plasma concentration-time curve;  $\text{AUC}_{(0-t)}$ , area under the plasma concentration-time curve from time of dosing to time of last measurable concentration; CL/F, clearance;  $C_{\text{max}}$ , maximum concentration; GABA, gamma-aminobutyric acid; Ht, hematocrit; HPLC, high performance liquid chromatography; MTD, maximum tolerated dose; TFA, trifluoroacetic acid;  $t_{\text{max}}$ , peak time; V/F, distribution volume.

## ABSTRACT

This study was designed to investigate the human absorption, disposition and mass balance of  $^{14}\text{C}$ -brivaracetam, a novel high affinity SV2A ligand with potent anticonvulsant activity. Six healthy male subjects received a single oral dose of  $^{14}\text{C}$ -brivaracetam (150 mg, 82  $\mu\text{Ci}$  or 3.03 MBq). Serial blood and complete urine and feces were collected until 144 h post-dose. Expired air samples were obtained until 24h. Brivaracetam was rapidly absorbed, with  $C_{\text{max}}$  of 4  $\mu\text{g/mL}$  occurring within 1.5 h of dosing. Unchanged brivaracetam amounted to 90% of the total plasma radioactivity, suggesting a modest first pass effect. Plasma protein binding of radioactivity was low (17.5%). Urinary excretion exceeded 90% after 2 days and the final mass balance reached 96.8% of the radioactivity in urine and 0.7% in feces. Only 8.6% of the radioactive dose was recovered in urine as unchanged brivaracetam, the remainder being identified as non-CYP and CYP dependent biotransformation products resulting from hydrolysis of the amide moiety (M9, 34.2%), hydroxylation of the n-propyl side chain (M1b, 15.9%), and a combination of these two pathways leading to the hydroxyacid (M4b, 15.2%). Minor amounts of taurine and glucuronic acid conjugates and other oxidized derivatives were also identified. Brivaracetam is completely absorbed, is weakly bound to plasma proteins, extensively biotransformed through several metabolic pathways and eliminated renally.

## INTRODUCTION

Brivaracetam is a novel ligand of the synaptic vesicle protein SV2A with a 10-fold higher affinity than levetiracetam (Kenda et al., 2004). A correlation between binding affinity for the SV2A site and anti-seizure protection in the mouse audiogenic seizure model has been demonstrated for a series of levetiracetam analogues (Lynch et al., 2004). Furthermore, brivaracetam dose-dependently inhibits voltage-dependent sodium currents (Zona et al., 2004) and reverses the inhibitory effects of negative modulators on gamma-aminobutyric acid (GABA)- and glycine-induced currents (Rigo et al., 2004). Preclinical *in vivo* and *in vitro* studies with brivaracetam have demonstrated that it induces a more potent and complete suppression of seizure activity in experimental models of epilepsy (Kenda et al., 2004; Matagne et al., 2003). Brivaracetam revealed pharmacological activity with ED<sub>50</sub> in the range of 1.2-2.6 mg/kg administered intraperitoneally in three rodent models of epilepsy (corneal-kindled mice, audiogenic susceptible mice and Genetic Absence Rats from Strasbourg) (Matagne et al., 2003), corresponding to predicted human equivalent doses of 70-160 mg/day using bodyweight or 6-25 mg/day using body surface extrapolation. The clinical safety, tolerability and pharmacokinetics of brivaracetam have been extensively studied in healthy human subjects (Rolan et al., 2004; Sargentini-Maier et al., 2007). The maximum tolerated dose (MTD) was 1000 mg after single oral dose and >800 mg/day after two weeks of multiple dosing. Brivaracetam was rapidly absorbed orally, food did not affect the extent of absorption, its distribution volume amounted to the total volume of body water and plasma half-life was between 7 and 8 hours (Rolan et al., 2004; Sargentini-Maier et al., 2007). A proof of concept study in photosensitive epileptic patients confirmed the potent

antiepileptic activity of the compound (Kasteleijn-Nolst Trenité et al., in press), as evidenced by complete suppression of photoparoxysmal response lasting more than two days in all patients following a single dose of 80 mg.

The objectives of the present study were to characterize the absorption, metabolism, disposition and mass balance of a single 150 mg oral dose of  $^{14}\text{C}$ -brivaracetam in healthy male subjects.

## Materials and Methods.

### *Reference Substances and Chemicals*

Brivaracetam ((2S)-2-[(4R)-2-oxo-4-propylpyrrolidinyl] butanamide) (M7) and the metabolite synthetic standards, (2S)-2-[(4R)-2-oxo-4-(2-(R)-hydroxy-propyl)pyrrolidin-1-yl] butanamide (M1a), (2S)-2-[(4R)-2-oxo-4-(2-(S)-hydroxy-propyl)pyrrolidin-1-yl] butanamide (M1b), (2S)-2-[(4R)-2-oxo-4-(2-oxopropyl)pyrrolidin-1-yl] butanamide (M3) and (2S)-2-[(4R)-2-oxo-4-propylpyrrolidin-1-yl] butanoic acid (M9) were synthesized by UCB Pharma (Braine-l'Alleud, Belgium). [ $^{14}\text{C}$ ]-brivaracetam, labeled on the carbonyl position of the pyrrolidone ring, was obtained from Amersham Biosciences (Chalfont St Giles, Bucks, United Kingdom). Liquid scintillation cocktails were from Canberra-Packard Benelux (Zellik, Belgium). All other commercially available reagents and solvents were of either analytical or HPLC grade.

### *Clinical Study*

The study was conducted at the SGS Clinical Research Unit, Stuyvenberg Hospital, Antwerp (Belgium). The study protocol and the dosimetry calculations were approved by the Medical Ethics Committee of the public hospitals of the city of Antwerp. The trial was conducted according to the recommendations described in the declaration of

Helsinki. Written informed consent was obtained from each subject prior to the start of the trial, after being informed of the nature and implications of the study.

The tissue distribution in non pigmented and pigmented rats allowed to conclude that the oral administration of 2.9 MBq (79  $\mu$ Ci) of  $^{14}$ C-brivaracetam would result in a Committed Effective Dose of 0.1 mSv, placing this trial at the upper limit of Risk Category I (ICRP Publication 60, 1991; ICRP Publication 62, 1993), *viz.* one tenth of the maximum permissible dose in this type of trial (category IIa, 1 mSv).

Brivaracetam was dissolved in ethanol together with  $^{14}$ C-brivaracetam in suitable proportions to obtain a specific radioactivity of about 20 KBq/mg (0.54  $\mu$ Ci/mg). The solution was evaporated to dryness and 150 mg of powder was accurately weighed (to the nearest 0.1 mg) into hard gelatin capsules without excipients. The amount per capsule, the specific radioactivity of the labeled drug substance, the total radioactivity per capsule and the isotopic purity were controlled shortly before use.

After an overnight fast, six healthy male subjects took one capsule containing 150 mg  $^{14}$ C-brivaracetam with 240 mL water. The participants remained in upright position for 1 hour. Food was withheld until 4h post-dose. Standardized meals were provided according to a fixed schedule. The subjects remained confined in the unit for the first 8 days of the study or until at least 95% of the radioactive dose was excreted.

Blood samples were collected in heparin-containing tubes before dosing and at 0.25 h, 0.5 h, 1 h, 1.5 h, 2 h, 3 h, 4 h, 6 h, 9 h, 12 h, 24 h, 36 h, 48 h, 72 h, 96 h, 120 h, 144 h post-dose. For metabolite identification and *ex-vivo* radioactivity protein binding measurements, additional blood samples were collected from each subject at 1 h, 12 h and 24 h post-dose. Aliquots of 1 mL were kept for the determination of radioactivity in whole blood and the remainder was centrifuged at 4°C. Plasma

samples were obtained by centrifugation (10 minutes, 2000 g, 4°C), and transferred into polypropylene tubes for the determination of total radioactivity, for the determination of the parent compound and for metabolic profiling. Hematocrit was determined once daily, in the morning. Expired air was collected at pre-dose, 0.5 h, 1 h, 1.5 h, 2 h, 3 h, 4 h, 6 h, 9 h, 12 h and 24 h post-dose: subjects were requested to blow through a glass straw into a vial containing 4 mL of a 1:1 mixture of Hyamine 10X hydroxide and of 96% ethanol containing 0.02% phenolphthalein, until persistent bleaching of the indicator. The amount of alkaline reagent was calculated to trap 1 mmol of carbon dioxide. Cumulative excretion was calculated assuming a carbon dioxide production of 1 kg/day or 947 mmol/hour in man.

All urine emissions were collected in fractions at predetermined intervals: pre-dose, 0-6 h, 6-12 h, 12-24 h, 24-48 h, 48-72 h, 72-96 h, 96-120 h and 120-144 h. All post-dose stools were collected in stomacher bags (Seward Medical, London, United Kingdom) placed in tared plastic jars. Blood and air samples were stored at +4°C and all other samples at -20°C until submitted to analytical determinations.

### *Radioactivity Determinations*

Radioactivity in blood, plasma, urine, feces and expired air was determined using a liquid scintillation counter (Tri-Carb model 2900TR, Canberra-Packard Benelux, Zellik, Belgium). The total radioactivity in plasma and blood was expressed as microgram-equivalents ( $\mu\text{g-eq}$ )/mL brivaracetam. For plasma and urine samples, two aliquots (0.5 mL and 1.0 mL, respectively) were mixed directly with 10 mL Ultima Gold scintillation cocktail followed by liquid scintillation counting. For expired air, the vials containing the trapped air were added with 9 mL of Hionic-Fluor and the samples were counted. Feces were mixed with water (ca. 1:1) and homogenized

using a Stomacher 400 apparatus (Seward Medical). At least four aliquots of fecal homogenates (ca. 100 mg) were combusted using a Sample Oxidizer model 307 (Canberra-Packard). Radioactivity in the combustion products was determined by trapping the liberated  $^{14}\text{CO}_2$  in various proportions of Carbo-Sorb-E absorbing reagent, followed by liquid scintillation counting using Permafluor E scintillation cocktail. For blood samples, two 0.25 mL aliquots were combusted and measured in a similar manner to that of the fecal homogenates. The radioactivity in blood cells was calculated from hematocrit (Ht) and from whole blood and plasma radioactivity using the equation:  $C_{\text{cell}} = [C_{\text{blood}} - C_{\text{plasma}} \times (1 - \text{Ht})] / \text{Ht}$ .

#### *Determination of Plasma Protein Binding*

The *ex-vivo* plasma protein binding of radioactivity was determined by equilibrium dialysis. Plasma samples (1 mL) were dialyzed in triplicate at 37°C during 4h using a Dianorm dialysis apparatus (Diachema AG, Zurich, Switzerland) and Spectra/Por membranes (membrane area= 4.5 cm<sup>2</sup>; molecular weight cut-off= 12000-14000, Spectrum Inc., Houston, TX, USA). Dialyzed plasma and buffer were mixed with 10 mL Emulsifier Scintillator Plus scintillation cocktail and submitted to liquid scintillation counting. The percent binding of radioactivity to plasma proteins was expressed as follows:  $\text{Binding}(\%) = 100 \times (C_{\text{plasma}} - C_{\text{buffer}}) / C_{\text{plasma}}$ .

#### *Quantification of Brivaracetam in Plasma*

Brivaracetam was determined in plasma samples after pre-purification on solid phase extraction cartridges, using a previously described liquid chromatography mass spectrometry method with electrospray ionization (LC/ESI/MS) (Sargentini-Maier et al, 2007). The lower limit of quantification was 0.05 µg/mL.



### *Sample Preparation for Metabolite Profiling and Structural Elucidation*

Plasma samples (1 mL) were diluted with 1 mL of water containing 0.2% v/v trifluoroacetic acid (TFA), vortexed, diluted with 1 mL of methanol, vortexed and diluted again with 1 mL acetonitrile. After centrifugation and separation of the supernatant, the pellet was washed. The supernatant and the pellet wash were subsequently pooled, evaporated to dryness and the residue reconstituted with 500  $\mu$ L of water, containing 5% v/v acetonitrile, prior to analysis. Urine samples were centrifuged to remove insoluble material prior to analysis.

### *Metabolic Profiling*

All urine samples from 0-6h, 6-12h, 12-24h and 24-48h post-dose and all plasma samples until 24h post-dose were analyzed individually, as collected. The radio-HPLC system consisted of an Agilent 1100 series chromatograph (Agilent Technologies, Diegem, Belgium) coupled to a Radiomatic 515 TR radiochemical detector (Canberra-Packard). The separation was performed on an Inertsil ODS-3 column (250 x 4.6 mm, 5  $\mu$ m, GL Sciences, Tokyo, Japan) protected by an Inertsil ODS-3 guard column, thermostatically regulated at 40°C. The eluents were (A) 0.1% aqueous TFA (adjusted to pH 2.4 with aqueous ammonia) and 5% acetonitrile and (B) 0.1% aqueous TFA (pH 2.4) and 90% acetonitrile, at a total flow rate of 1 mL/min. A gradient was programmed from 0 to 35% of B in 70 minutes followed by 15 minutes at 100% B. A UV detector (220 nm) was inserted upstream of the radiochemical detector, for recording retention times of the reference standards. The radiochemical detector cell had a volume of 1 mL for urine and of 2 mL for plasma, and received Ultima-Flo M scintillation cocktail at a flow rate of 3 mL/min. The background to be subtracted ( $B_s$ ) from a radio-HPLC analysis was evaluated as follows :  $B_s = [B_m / N$

+ 2 x (Bm/N)<sup>0.5</sup>] x N, where Bm is the measured background and N the number of samplings per minute. For the reported analyses, the measured backgrounds for the different counting cells were 9.4 cpm (1 mL counting cell) and 14.2 cpm (2 mL counting cell). The corresponding subtracted backgrounds were 28.8 cpm and 38.0 cpm. The efficiency has been checked to be constant over the entire gradient (i.e. RSD = 2.4%). The minimum detectable activity (MDA) was calculated as follows: MDA = Bm x Peak width / Tr, where Tr is the residence time in the counting cell. In plasma and urine, the MDA was 82.4 cpm and 109 cpm, respectively.

#### *Metabolite Structural Elucidation*

The mass spectrometer was a Micromass tandem quadrupole time-of-flight QTOF2 instrument (Micromass, Manchester, UK) with dual electrospray source, operated by the Masslynx version 4.0 data system. In full positive ion mode, the sample spray cone voltage was set at 20 V. The collision energy was 10 eV for full scan MS and CID experiments. In CID mode the resolution of the quadrupole filter was set to approximately 5 a.m.u. to enable the entrance of a complete isotope cluster into the collision hexapole. The HPLC system was operated under the same conditions as described for metabolic profiling.

Metabolites were identified by the accurate masses of their protonated molecular ion and of fragment ions generated in-source or by CID. Compounds M1a, M1b, M3, M7 and M9 were confirmed by comparison of their retention times with authentic reference standards.

Metabolite M4b was isolated and purified from 250 mL of 12-24h urine from subject 2 and its structural identification was performed by <sup>1</sup>H nuclear magnetic resonance.

The 250 mL urine sample was mixed with an equal volume of 0.1% aqueous TFA. An Oasis HLB SPE column (Waters Corp., Milford, USA) containing 6 g of packing was conditioned successively with 70 mL of MeOH and 35 mL of 0.1% aqueous TFA. The 500 mL of diluted urine were slowly loaded onto the SPE column. The radioactive peak of interest was not retained on the column and eluted in the effluent. The latter was adjusted to pH 2.4 with aqueous 20% TFA and re-loaded on a conditioned 6 g Oasis HLB SPE column. The column was washed out with 20 mL of water containing 0.1% TFA. The metabolite was then eluted with 30 mL of acetonitrile/methanol 70:30, which was evaporated to dryness under vacuum. The residue was reconstituted in 5 mL of 5% acetonitrile in 0.1% aqueous TFA pH 2.4. The sample was then subjected to semi-preparative HPLC on an Inertsil ODS-3 (250 x 10 mm, 5  $\mu$ m) column at a temperature of 40°C, using the same gradient system as for metabolic profiling and a flow rate of 2.5 mL/min. Fractions were collected using an Agilent 220 fraction collector. Each fraction was counted by LSC and individually analyzed by radio-HPLC. The fractions of interest were reduced under nitrogen to 1 mL and reinjected, and the purified metabolite was collected from the column effluent while monitoring the signal of the radiometric detector fitted with a 150  $\mu$ L heterogeneous counting cell. The purity of the final fraction was checked by HPLC with radiometric and UV detection. The final sample was evaporated to dryness under nitrogen and reconstituted in deuterated acetonitrile. Structural determination was performed by  $^1$ H nuclear magnetic resonance spectrometry on a Bruker DRX-400 MHz spectrometer.

### *Pharmacokinetic Analysis*

Pharmacokinetic parameters were derived using standard non-compartmental methods (Kinetica 2000, version 3.0, Innaphase, Champ sur Marne, France).

Maximum concentration ( $C_{\max}$ ) and peak time ( $t_{\max}$ ) were directly derived from the concentration-time profiles. The area under the plasma concentration-time curve from the time of dosing to the time of the last measurable concentration ( $AUC_{(0-t)}$ ) was calculated by the linear trapezoidal rule and extrapolated to infinity (AUC) as  $AUC_{(0-t)} + Ct/\lambda_z$ , in which  $\lambda_z$ , the first order rate constant associated with the terminal elimination phase, was estimated by linear regression of time versus log concentration. The apparent half-life ( $t_{1/2}$ ) of the terminal elimination phase was calculated as  $\ln(2)/\lambda_z$ . The total amount of excreted radioactivity was the sum of the amount excreted in urine, feces and air.

## Results

The six male subjects who participated in the study had a mean age of 30.9 years (range: 18.5-43.8 years) and a mean body weight of 78 kg (range 69-92 kg). The administered brivaracetam and radiocarbon doses were  $150.2 \pm 5.3$  mg (mean  $\pm$  standard deviation,  $n=6$ ) and  $3.02 \pm 0.11$  MBq ( $81.6 \pm 3$   $\mu$ Ci). The radiochemical purity of brivaracetam was found to be 100%.

### *Mass Balance*

The cumulative recovery of radiocarbon reached  $97.5 \pm 0.7$  % of the dose in 144 h (Table 1). Most of the radioactivity was recovered in urine ( $96.8 \pm 0.7$  %) and less than 1% in feces. No radioactivity was detected in exhaled air. The mean cumulative recovery of total radioactivity in urine over time is graphically illustrated in Fig. 1.

### *Pharmacokinetics*

The mean plasma concentration-time profiles of radiocarbon and unchanged brivaracetam are illustrated in Fig. 2. The peak plasma concentration was reached at 1.5 h post-dose for both brivaracetam and radiocarbon (Table 2a). The area under the radiocarbon concentration curve,  $49.8 \pm 8.30$   $\mu\text{g eq/mL}$ , was only slightly higher than for unchanged brivaracetam,  $44.6 \pm 11.3$   $\mu\text{g/mL}$  (Table 2a). The mean apparent half-lives ( $t_{1/2}$ ) were also similar, *viz.*  $8.8 \pm 1.5$  h and  $7.6 \pm 1.7$  h respectively. The clearance (CL/F) and distribution volume (V/F) of brivaracetam were  $0.77 \pm 0.19$  mL/min/kg and  $0.49 \pm 0.05$  L/Kg. The ratios of blood cell to plasma radioactivity versus time were submitted to linear least squares regression: the mean ( $\pm$ SD) intercept and slope were  $0.58 \pm 0.07$  and  $0.002 \pm 0.003$  ( $n=6$ ).

### *Metabolite Profiling.*

The recovery for the urine sample preparation step was checked on early and late samples and found to be >95%. Similarly, the extraction recovery for plasma was >90%. The column recovery at the end of the gradient was 100% for both plasma and urine.

As evidenced in Table 2b, brivaracetam was the predominant species in plasma at 1.5, 6 and 12 h post-dose, amounting to *ca.* 90% of the total circulating radioactivity. Metabolite M9 was measurable in some individuals up to 6 h post-dose and accounted for less than 10% of the circulating radioactivity, while metabolite M1b appeared later and reached 6% of the circulating radioactivity at 12 h (15.5% in one individual). Metabolites M3 and M4b were below the limit of detection at all times (minimum detectable radioactivity 82.4 cpm). A representative HPLC

radiochromatogram of circulating metabolites is shown in Fig. 3a (subject 2, 6 h post-dose sample).

Table 3 lists the mean percentages of each brivaracetam-related species excreted in the urine in the 0-48 hour time interval, together with their assigned structure and characteristic molecular ions and two main fragmentation products. A representative radiochromatogram of urine (subject 2, 6-12 hours time interval) is shown in Fig. 3b.

The mean 48 h cumulative urinary excretion of the parent compound M7 was  $8.6 \% \pm 3.8$  of the dose, whereas that of M9, M1b and M4b amounted to  $34.2 \pm 6.1$ ,  $15.9 \pm 7.4$  and  $15.2 \pm 2.4$  % of the dose, respectively. All other metabolites (M1a, M2, M3, M4a, M5, M6 and M8) were minor, each of them amounting for less than 5% of the dose.

#### *Metabolite Identification.*

In addition to the parent drug, ten metabolites were identified in the urine (Table 3).

*Brivaracetam (M7)* exhibited an  $MH^+$  molecular ion at  $m/z$  213. Fragment ions at  $m/z$  196 and 168, issued respectively from a loss of  $NH_3$  and  $NH_3+CO$ , indicated the presence of an amide group. Its identity was confirmed by comparison with the reference standard.

*Metabolites M1a and M1b* displayed a protonated molecular ion at  $m/z$  229, 16u higher than the parent drug, suggesting isomeric monohydroxylated metabolites. Their full scan mass spectra displayed the class-characteristic losses of an intact amide group with elimination of  $NH_3$  at  $m/z$  212 followed by a consecutive loss of CO to generate a signal at  $m/z$  184. The high resolution mass to charge ratios of the

molecular ion and of the characteristic fragments were identical for M1a and M1b (Table 3).

*Metabolite M2* eluted in the front part of the M3 peak. The full scan mass spectrum of Metabolite M2 showed a protonated molecule at  $m/z$  243, 30u higher than the parent drug, suggesting the formation of a carboxylic acid group. Fragment ions at  $m/z$  226 and 198, issued respectively from a loss of  $\text{NH}_3$  and  $\text{NH}_3+\text{CO}$  indicated that the amide group present on the parent drug was intact. The CID product ion mass spectrum of the deprotonated molecule ( $m/z$  241) suggested the presence of a carboxylic acid group on the propyl chain. Accurate mass measurement results in CID mode revealed class-characteristic losses of  $\text{H}_2\text{O}$  ( $m/z$  223) and  $\text{CO}_2$  ( $m/z$  197) from the deprotonated molecule and indicated a carboxylic acid group. Moreover an abundant fragment ion at  $m/z$  127 indicated an intact butyramide moiety. Based on these data, M2 was tentatively identified as 2-[4-(3-carboxypropyl)-2-oxo-pyrrolidin-1-yl]-butyramide.

*Metabolite M3* exhibited a protonated molecular ion at  $m/z$  227, 14u higher than the parent drug, suggesting conversion of a  $\text{CH}_2$  of the parent drug to a ketone. The full scan mass spectrum indicated the class-characteristics losses of an intact amide group with elimination of  $\text{NH}_3$  at  $m/z$  210 along with a consecutive loss of  $\text{CO}$  at  $m/z$  182. Based on these data, M3 was identified by comparison with the reference standard as incorporating the ketone group on the penultimate carbon of the propyl chain.

*Metabolites M4a and M4b* displayed a protonated molecular ion at  $m/z$  230. 17u higher than the parent drug, suggesting isomeric monohydroxylated metabolites with the amide group hydrolyzed. Fragment ions at  $m/z$  212 and 184, issued respectively

from a loss of H<sub>2</sub>O and H<sub>2</sub>O+CO, indicated that the amide present on the parent drug had been hydrolyzed. The structure of metabolite M4b was also confirmed by high field NMR following preparative chromatography isolation from urine and purification.

The 400 MHz <sup>1</sup>H, <sup>1</sup>H-COSY spectrum of metabolite M4b is displayed in Fig. 4. The triplet at δ = 0.9 ppm and the doublet at δ = 1.1 ppm were assigned to methyl groups. By its multiplicity, the doublet indicated that it had only one vicinal proton and thus that the monohydroxylation took place on the penultimate carbon of one of the alkyl chains. That vicinal proton was identified as the sextuplet at δ = 3.7 ppm by a cross peak in the COSY spectrum. It was coupled to a triplet at δ = 1.5 ppm as indicated by a cross peak in the COSY spectrum. From its multiplicity and chemical shift, that signal was assigned to the methylene in position 1 on the propyl chain confirming that the hydroxylation took place on the propyl chain in ω-1 position. From the COSY spectrum it can be seen that that triplet was integrated in the 2-oxo-4-propylpyrrolidinyl spin system. The second spin system of the molecule was associated to the unchanged butyramide chain. The particularity in that COSY spectrum was the doublet at δ = 1.3 ppm correlated with the sextuplet at δ = 5.2 ppm. Those were respectively assigned to the methyl and the methine of the alcohol moiety of a first molecule of M4b forming an ester link with a second molecule of M4b. This dimer was found to be stable in pure acetonitrile but unstable in water. Based on these data, M4b was identified as the 2-[2-oxo-4-(2-hydroxypropyl)pyrrolidin-1-yl]butanoic acid. By analogy with the metabolites M1a and M1b, M4a was tentatively identified as the diastereoisomer of M4b.

*Metabolite M5* displayed a full scan mass spectrum with a protonated molecular ion at *m/z* 228, 15 u higher than the parent drug, suggesting hydrolysis of the amide



group and conversion of a CH<sub>2</sub> of the parent drug to a ketone. Fragment ions at *m/z* 210 and 182, issued respectively from a loss of H<sub>2</sub>O and H<sub>2</sub>O+CO, suggested that the amide group of the parent drug had been hydrolyzed. The CID product ion mass spectrum of the deprotonated molecule M5 displayed a loss of acetone, indicating that the ketone group was on the penultimate carbon of the propyl chain. Based on these data, M5 was tentatively identified as 2-[2-oxo-4-(2-oxo-propyl)pyrrolidin-1-yl]butanoic acid.

*Metabolite M6* displayed a protonated ion at *m/z* 321, 107u higher than the carboxylic acid metabolite M9, suggesting a taurine conjugate. The full scan mass spectrum displayed the class-characteristic fragment ions at *m/z* 196 issued from the loss of the taurine moiety, and at *m/z* 168 issued from a subsequent loss of CO. From these data M6 has been tentatively identified as the taurine conjugate of M9.

*Metabolite M8* exhibited a protonated molecular ion at *m/z* 390, 176u higher than the metabolite issued from amide hydrolysis M9, suggesting a glucuronide conjugate. The full scan mass spectrum indicated the class-characteristic fragment at *m/z* 214 issued from the loss of dehydroglucuronic acid (-176u) and 168, from the loss of CO. Based on these data, M8 was tentatively identified as an ester glucuronide of M9.

*Metabolite M9* displayed a protonated molecular ion at *m/z* 214, 1u higher than the parent drug, suggesting the hydrolysis of the amide group to a carboxylic acid. Fragment ions at *m/z* 196 and 168, issued respectively from a loss of H<sub>2</sub>O and H<sub>2</sub>O+CO, indicated that the amide group present on the parent drug had been hydrolyzed. M9 was also identified by comparison with the reference standard. The overall biotransformation scheme of brivaracetam is illustrated in Fig. 5.

### *Ex-vivo Protein Binding*

The non specific binding of radioactivity to the dialysis apparatus appeared to be insignificant and the time to reach equilibrium was 4 hours. The concentrations of radioactivity in the analyzed plasma ranged from 410 to 3600 ng eq/mL: within this concentration range the protein binding was independent of the initial concentration. The average (SD) plasma protein binding at 1 h, 12 h and 24 h post-dose was  $18.7 \pm 1.7$  %,  $17.6 \pm 2.0$  % and  $16.2 \pm 3.5$  % respectively.

### **Discussion**

The objective of the present study was to characterize the absorption, metabolism, disposition and mass balance of a single 150 mg oral dose of radiocarbon-labeled brivaracetam, and to identify its biotransformation pathways in man. Mass balance was achieved, with a mean total recovery of radioactivity of 97.5%. Radioactivity was almost completely excreted in urine, accounting for 96.8% of the dose, whereas the radioactivity excreted in feces was <1%. No radioactivity was detectable in exhaled air.

Brivaracetam accounted for only 8.6% of the dose excreted in urine, indicating extensive biotransformation. However, unchanged brivaracetam represented the predominant circulating component (plasma AUC ratio to radioactivity ~90%).

The mean blood cell-to-plasma radioactivity ratio of 0.58 and the negligible change over time (~10% in 24 h) suggested some distribution in blood cells, reaching rapid equilibrium, and the absence of accumulation of brivaracetam or metabolites.

The plasma protein binding, 17.5% on average, was neither concentration nor time dependent. Since the bulk of plasma radioactivity was assigned to brivaracetam, this figure closely approximates the protein binding of the unchanged drug.

*In vitro* studies have shown that brivaracetam is slowly oxidized by liver microsomes and human hepatocytes (Whomsley et al., 2007). In this study, ten metabolites issued from hydrolysis, oxidation and conjugation of brivaracetam were identified. Brivaracetam (M7) and four metabolites for which authentic standards were available (M1a, M1b, M3, and M9) were confirmed by their chromatographic retention times and high resolution mass spectra. The structure of M4b was assigned based on high resolution mass spectral and proton NMR data. By analogy with M1a/M1b, M4a was tentatively identified as the diastereoisomer of M4b. The chemical structures of other metabolites were tentatively assigned based on mass spectral data only.

The proposed scheme for the biotransformation pathways of brivaracetam in man is illustrated in Fig. 5. The major route of metabolism is the hydrolysis of the acetamide moiety leading to the carboxylic acid metabolite M9 (34% of the dose in urine). The other major metabolic pathways are the oxidation of the propyl-chain leading to M1b (16% of the dose in urine) and the product of the hydrolysis of M1b and/or oxidation of M9 to M4b (15% of the dose in urine). Other oxidized metabolites (M3 and M5) and conjugates with glucuronic acid (M8) or taurine (M6) played a minor role in the biotransformation of brivaracetam. Overall, the identified metabolites accounted for >87% of the radioactivity recovered in urine.

In human liver microsomes, the *in vitro* and *in vivo* intrinsic clearance for production of M1b from brivaracetam were low. The extrapolated hepatic clearance (0.16 mL/min/kg) represented only 20% of the total *in vivo* clearance suggesting a

low potential for interference with brivaracetam metabolism through inhibition of CYP-mediated metabolism. The principal CYP isoform responsible for the production of M1b is CYP2C8, with minor contributions from CYP3A4, CYP2C19 and possibly CYP2B6 (Whomsley et al., 2007).

The enzymes responsible for the production of the acidic metabolites M9 and M4b are unknown although it is speculated that the hydrolysis of the acetamide moiety is mediated by high capacity/low affinity amide hydrolases similarly to levetiracetam, another member of the racetam family (Strolin Benedetti et al., 2003). Whether the hydroxy acid M4b is formed by hydrolysis to M9 followed by oxidation, or by oxidation to M1b followed by hydrolysis is also unknown and deserves further investigation.

In conclusion, this study has shown that brivaracetam is completely absorbed, is weakly bound to plasma proteins, is extensively metabolized through several non-CYP and CYP dependent pathways and is entirely eliminated renally. The biotransformation of brivaracetam is therefore unlikely to be importantly altered by clinical drug interactions. However, characterization of the enzymes involved in its metabolism warrants further investigations.

### **Acknowledgments**

The authors are grateful to M. Plisnier, B. Mathieu, P. Jacques, D. Tytgat and A. Vandebosche (SGS) for their skilful contribution to mass spectrometry, radio-analytical and nuclear magnetic resonance experiments, and acknowledge with thanks the role of the clinical investigator Dr. S. Ramael and his nursing staff.

## References.

ICRP Publication 60 (1991) 1990 *Recommendations of the International Commission on Radiological Protection*. Pergamon Press, Oxford.

ICRP Publication 62 (1993) *Radiological Protection in Biomedical Research*. Pergamon Press, Oxford.

Kasteleijn-Nolst Trenité DGA, Genton P, Parain D, Masnou P, Steinhoff BJ, Jacobs T, Pigeolet E, Stockis A, and Hirsch E (2007) Evaluation of brivaracetam, a novel SV2A ligand, in the photosensitivity model. *Neurology* (in press).

Kenda BM, Matagne AC, Talaga PE, Pasau PM, Differding E, Lallemand BI, Frycia AM, Moureau FG, Klitgaard HV, Gillard MR, Fuks B, and Michel P (2004) Discovery of 4-substituted pyrrolidone butanamides as new agents with significant antiepileptic activity. *J Med Chem* **47**:530-549.

Lynch BA, Lambeng N, Nocka K, Kensel-Hammes P, Bajjalieh SM, Matagne A, and Fuks B (2004) The synaptic vesicle protein SV2A is the binding site for the antiepileptic drug levetiracetam. *Proc Natl Acad Sci USA* **101**:9861-9866.

Matagne A, Kenda B, Michel P, and Klitgaard H (2003) UCB 34714, a new pyrrolidone derivative: comparison with levetiracetam in animal models of chronic epilepsy in vivo. *Epilepsia* **44 (Suppl.9)**:260-261.

Matagne A, Kenda B, Michel P, and Klitgaard H (2003) UCB 34714, a new pyrrolidone derivative, suppresses seizures epileptogenesis in animal models of chronic epilepsy in vivo. *Epilepsia* **44 (Suppl.8)**:53-54.

Rigo JM, Nguyen L, Hans G, Belachew S, Moonen G, Matagne A, and Klitgaard H (2004) UCB 34714: effect on inhibitory and excitatory neurotransmission. *Epilepsia* **45 (Suppl.3)**:56.

- Rolan P, Pigeolet E, and Stockis A (2004) UCB 34714: single and multiple rising dose safety, tolerability, and pharmacokinetics in healthy subjects. *Epilepsia* **45 (Suppl.7)**:314-315.
- Sargentini-Maier ML, Rolan P, Connell J, Tytgat D, Jacobs T, Pigeolet E, Riethuisen JM, and Stockis A (2007) Brivaracetam safety, tolerability, pharmacokinetics and CNS pharmacodynamic effects after 10 to 1400 mg single rising oral doses in healthy males. *Br J Clin Pharmacol* **63**:680-688.
- Strolin Benedetti M, Whomsley R, Nicolas JM, Young C, and Baltes E (2003) Pharmacokinetics and metabolism of 14C-levetiracetam, a new antiepileptic agent, in healthy subjects. *Eur J Clin Pharmacol* **59**: 621-630.
- Whomsley R, Brochot A, Dell'Aiera S, Delepine X, and Espié P (2007) Identification of the cytochrome P450 isoforms responsible for the hydroxylation of brivaracetam. *The AAPS Journal*, annual symposium abstract (in press).
- Zona C, Pieri M, Klitgaard H, and Margineanu D-G (2004) UCB 34714, a new pyrrolidone derivative, inhibits Na<sup>+</sup> currents in rat cortical neurons in culture. *Epilepsia* **45 (Suppl.7)**:146.

## Figure legends

FIG. 1. Mean cumulative urinary excretion of total radioactivity (●), brivaracetam (○), M1b (▼), M9 (□), M4a (■), sum of brivaracetam and metabolites (□) following 150 mg single oral dose of <sup>14</sup>C-brivaracetam (n=6)

FIG. 2. Mean plasma concentration-time profiles of total radioactivity and brivaracetam following 150 mg single oral dose of <sup>14</sup>C-brivaracetam (n=6)

FIG. 3. (a) Representative radiochromatogram of circulating radioactivity (plasma at 6 hours, subject 2). (b) Representative urine radiochromatogram (6-12 hours interval, subject 2). Y axis is effluent radioactivity in counts per minute (cpm) and X axis is elution time in minutes.

FIG. 4. 400 MHz <sup>1</sup>H, <sup>1</sup>H COSY spectrum of metabolite M4b after isolation and purification from urine. Annotated off-diagonal signals and dashed lines show proton-proton correlation. Solvent was CD<sub>3</sub>CN. Asterisks indicate a putative dimer of M4b.

FIG. 5. Proposed metabolic pathways of brivaracetam in man (mean % dose recovered in urine within 48 h).

TABLE 1.

*Individual and mean (SD) cumulative excretion of <sup>14</sup>C-brivaracetam (% dose) until 144 hours post-dose (n=6)*

	Subject						Mean (SD)
	1	2	3	4	5	6	
Urine	97.9	96.6	96.1	96.3	97.6	96.4	96.8 (0.7)
Feces	0.527	0.951	0.571	0.545	0.723	0.928	0.71 (0.19)
Air	ND	ND	ND	ND	ND	ND	-
Total	98.4	97.6	96.7	96.8	98.3	97.3	97.5 (0.7)

ND: not detected



TABLE 2

(a) Plasma pharmacokinetic parameters (mean±SD) of total radioactivity and brivaracetam after a single 150 mg oral dose of <sup>14</sup>C-brivaracetam (n=6)

(b) Radiometabolite quantification (% of plasma radioactivity – median, minimum-maximum) in plasma at 1.5, 6 and 12h

(a)

Parameter	Total radioactivity	brivaracetam
Cmax (µg/mL)	3.6 ± 0.4	4.0 ± 0.5
tmax (h) <sup>(1)</sup>	1.5 (0.25-2)	1.5 (0.25-2)
AUC(0-t) (µg/mL)	48.9 ± 7.9	43.4 ± 10.8
AUC (µg/mL)	49.8 ± 8.3	44.6 ± 11.3
CL/F mL/min/kg)	-	0.77 ± 0.19
Vz/F (mL/Kg)	-	0.49 ± 0.05
t1/2 (h)	8.8 ± 1.5	7.6 ± 1.7

<sup>(1)</sup> median (range)

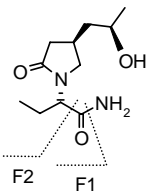
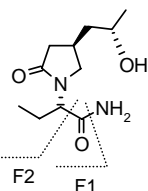
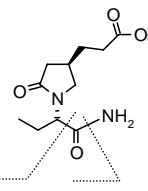
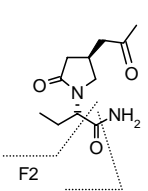
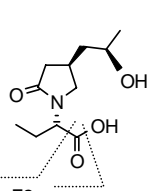
(b)

Compound	1.5 h	6 h	12 h
M1b	ND	ND (ND-8.4)	6.0 (ND-15.5)
M7 (brivaracetam)	96.7 (91.7-97.4)	91.0 (87.2-93.2)	88.8 (78.7-100)
M9	1.6 (ND-5.5)	3.2 (ND-6.7)	ND

ND: not detected (<82.4 cpm)

TABLE 3

Mean (SD, n=6) percentage of dose excreted in urine as radiometabolites over 48 hours, proposed chemical structure, and accurate mass of the MH<sup>+</sup> and MNa<sup>+</sup> molecular ions and two major daughter ions

Compound	% in 0-48h urine (SD)	Structures	Calculated mass and error (milliunits)			
			MH <sup>+</sup>	MNa <sup>+</sup>	F1	F2
M1a	0.2		229.1552 (0.7)	251.1372 (0.4)	212.1287 (0.5)	184.1338 (0.6)
M1b	15.9 (7.4)		229.1552 (0.9)	251.1372 (-1.1)	212.1287 (-0.4)	184.1338 (-0.2)
M2	Traces		243.1345 (3.1)	265.1164 (1.2)	226.1079 (0.9)	198.1130 (0.0)
M3	3.5		227.1396 (0.1)	249.1215 (0.2)	210.1130 (0.3)	182.1181 (-0.1)
M4a (tentative)	2.8		230.1392 (-0.2)	252.1212 (0.7)	212.1287 (0.8)	184.1338 (0.4)

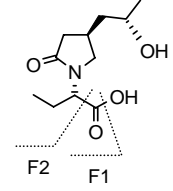
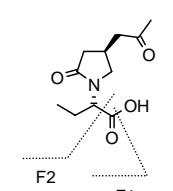
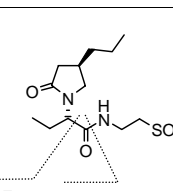
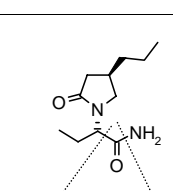
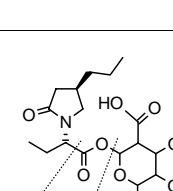
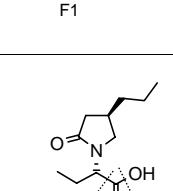
M4b	15.2 (2.4)		230.1392 (0.7)	252.1212 (0.9)	212.1287 (1.2)	184.1338 (1.6)
M5	3.8		228.1236 (1.8)	250.1055 (3.8)	210.1130 (2.5)	182.1181 (2.0)
M6	1.0		321.1484 (1.0)	343.1304 (2.2)	196.1338 (1.9)	168.1388 (3.3)
M7 (brivaracetam)	8.6 (3.8)		213.1603 (1.7)	235.1422 (-1.7)	196.1338 (-1.8)	168.1388 (-0.6)
M8	2.4		390.1764 (1.7)	412.1584 (2.3)	214.1443 (0.4)	168.1388 (1.5)
M9	34.2 (6.1)		214.1443 (-1.4)	236.1263 (0.4)	196.1338 (0.0)	168.1388 (-0.3)

Figure 1

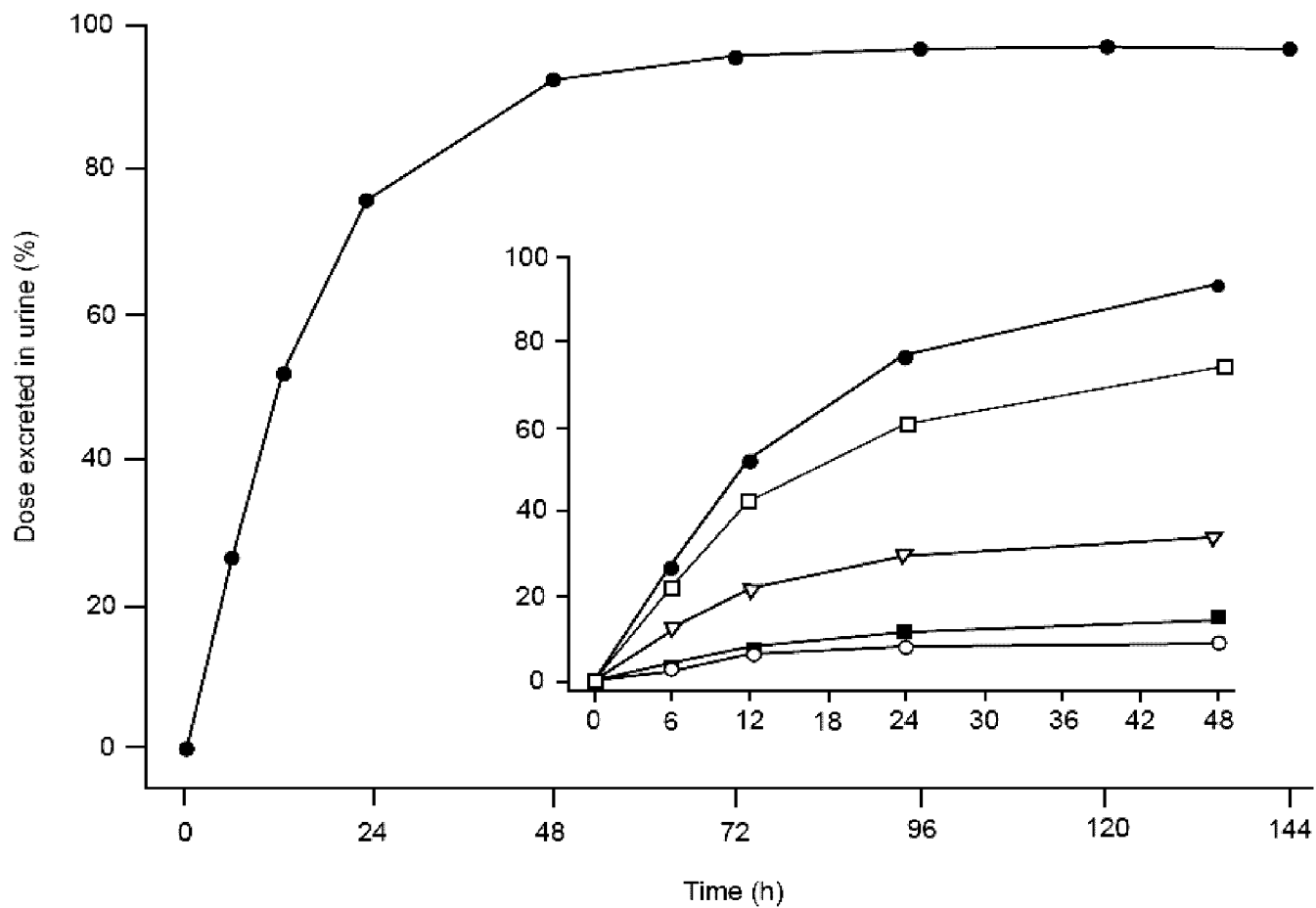


Figure 2

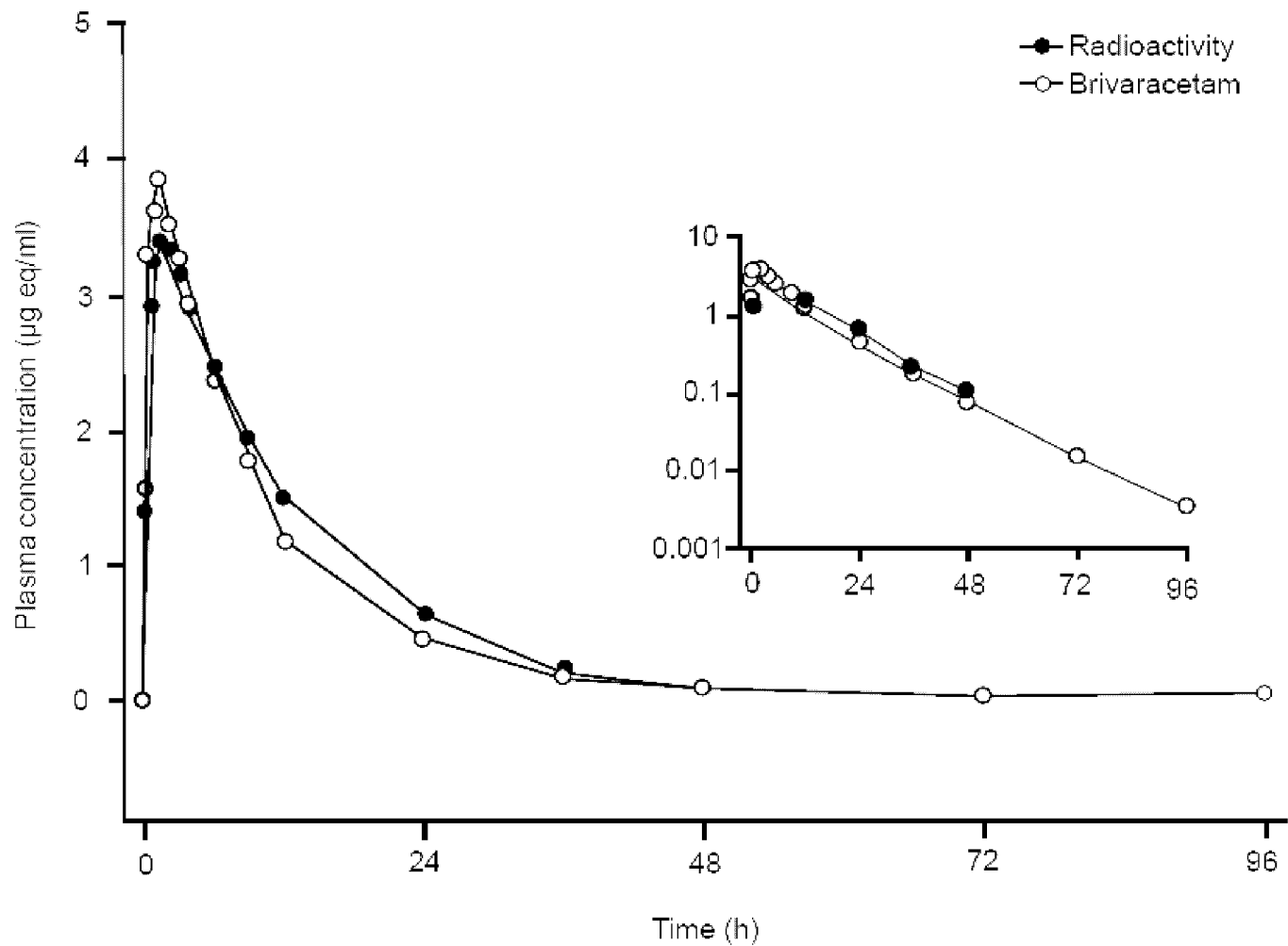


Figure 3a

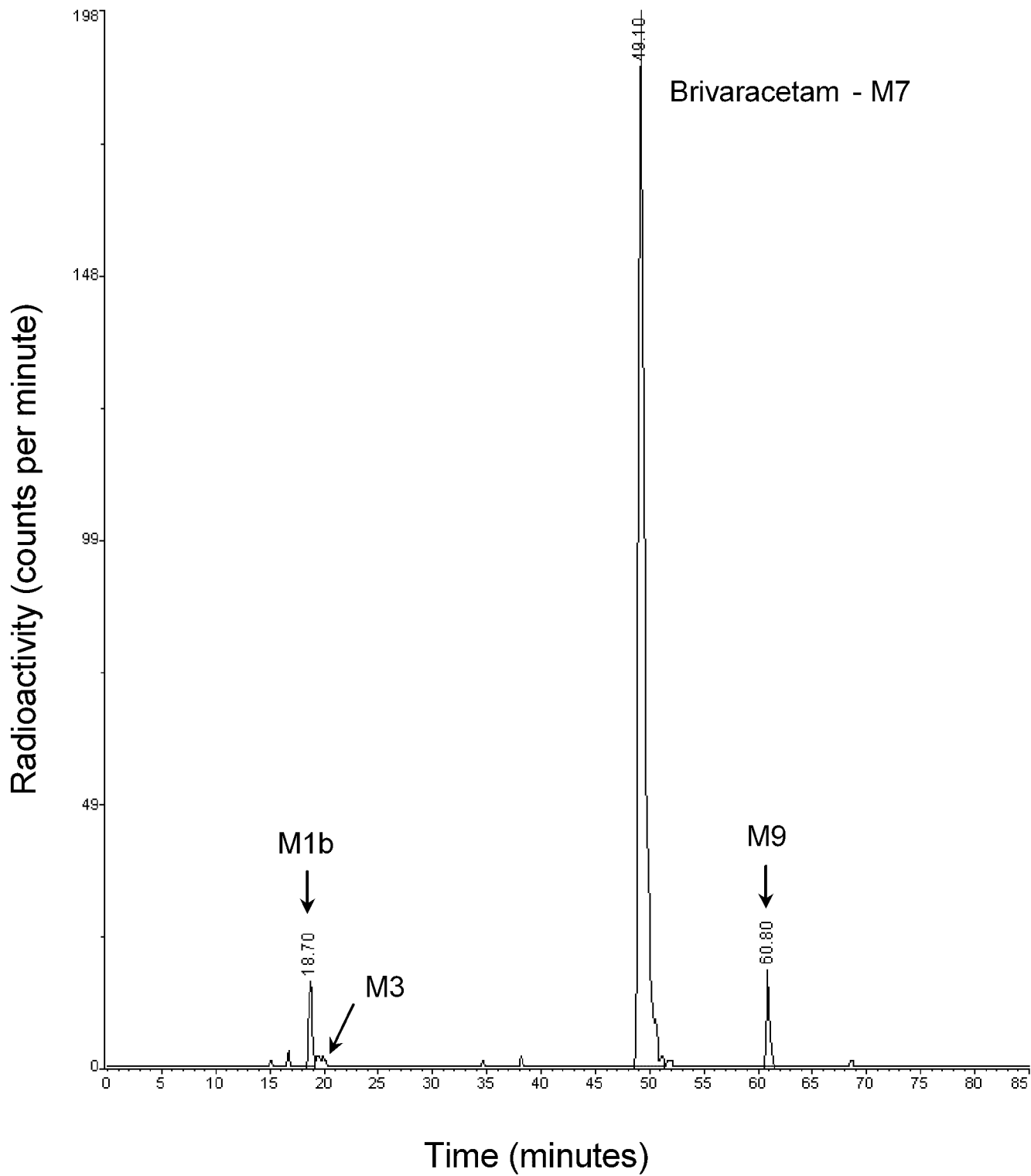


Figure 3b

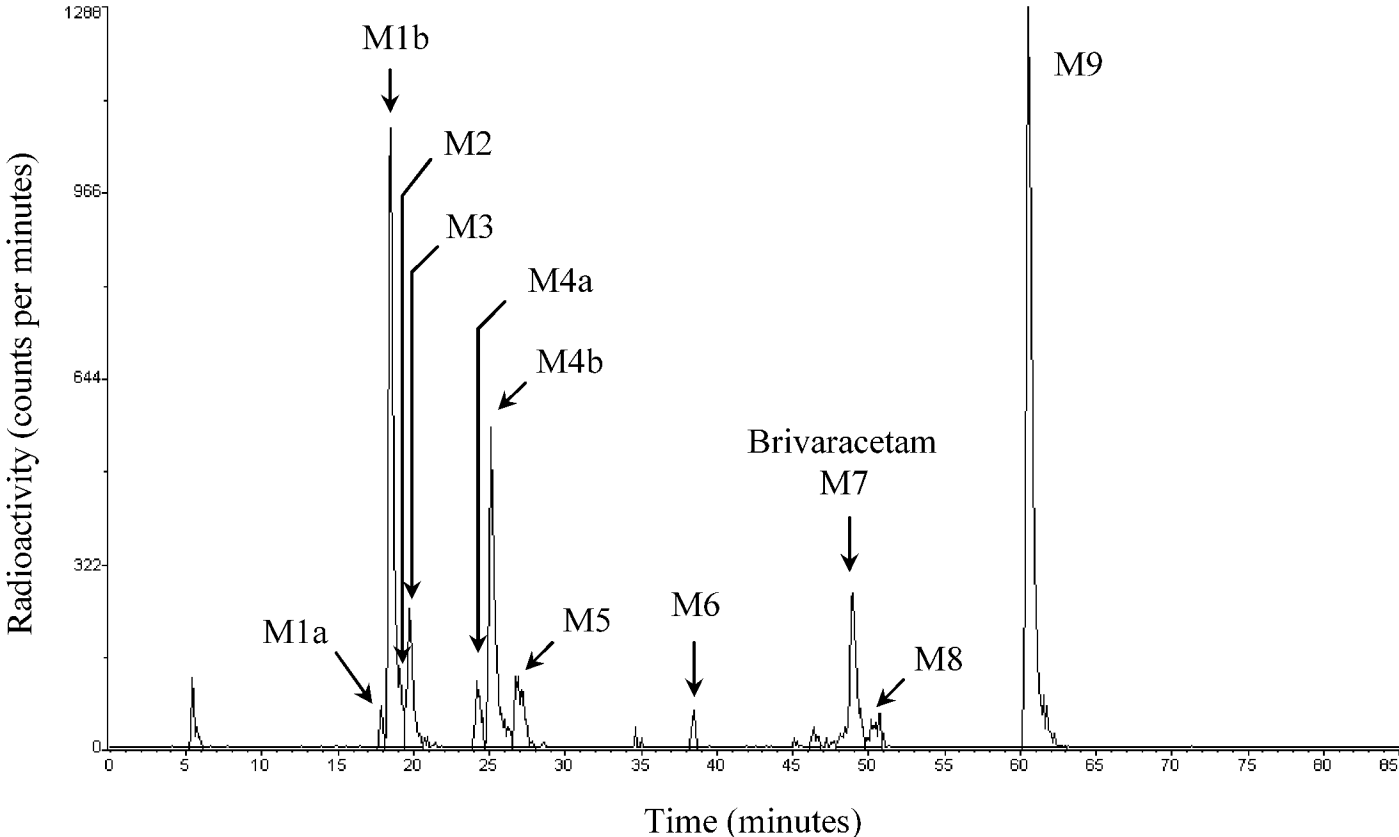


Figure 4

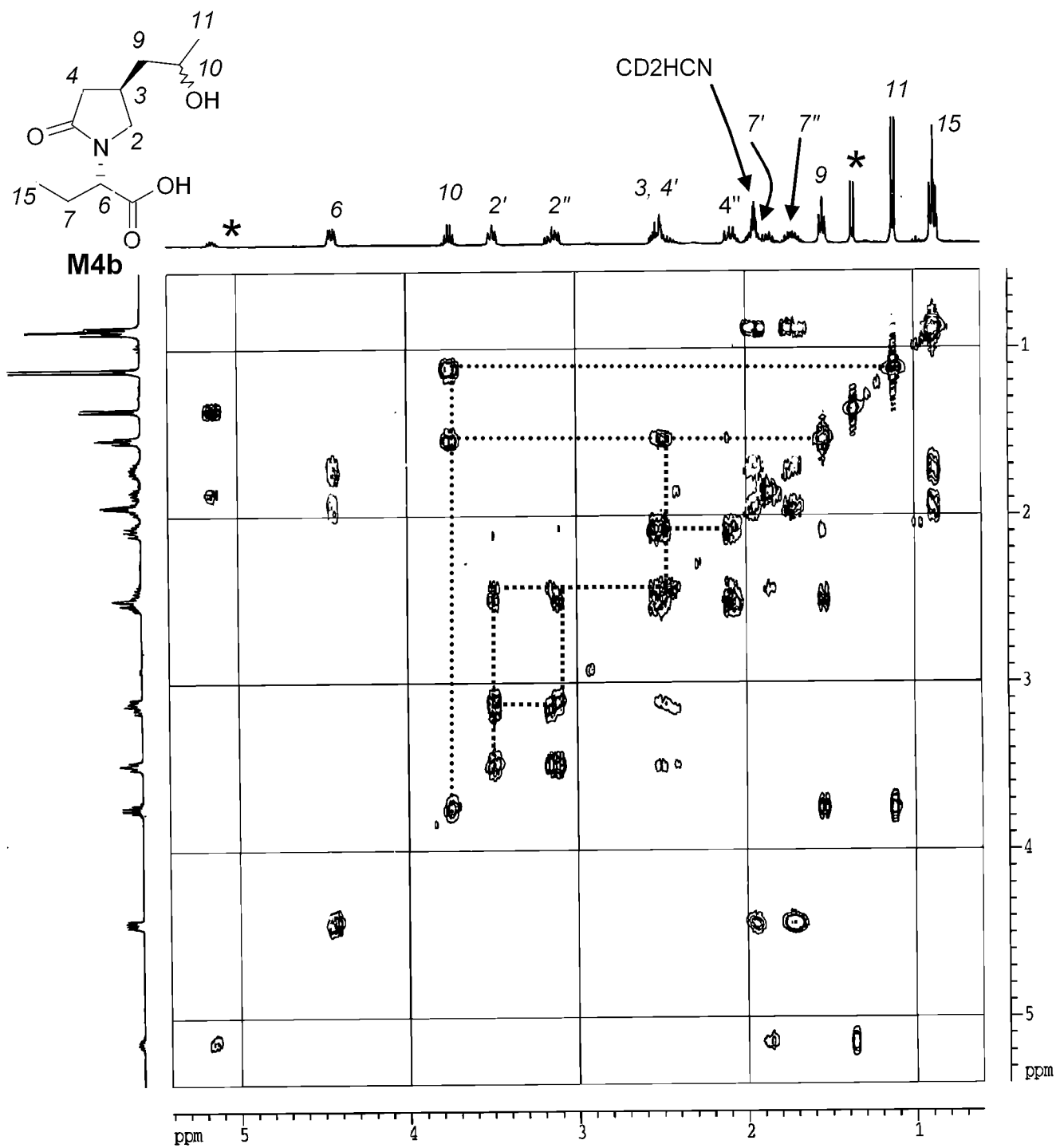




Figure 5

